

# Inhibiting effects of 5-substituted isatin-based Mannich bases on the corrosion of mild steel in hydrochloric acid solution

Ashish Kumar Singh · M. A. Quraishi

Received: 14 October 2009 / Accepted: 9 January 2010 / Published online: 23 January 2010  
© Springer Science+Business Media B.V. 2010

**Abstract** The inhibition effect of all the three Mannich bases against the corrosion of mild steel in 1 M HCl solution was studied by weight loss, electrochemical impedance spectroscopy (EIS), potentiodynamic polarization, and atomic force microscopy techniques. Data obtained from EIS studies were analyzed to model the corrosion inhibition process through appropriate equivalent circuit models. The adsorption of Mannich bases obeyed Langmuir adsorption isotherm. Both thermodynamic and activation parameters were calculated and discussed. Polarization curves indicate that they are mixed type of inhibitors. All the Mannich bases were adsorbed physically at lower concentration, whereas chemisorption was favored at higher concentration. The results obtained from weight loss, EIS, and Potentiodynamic polarization are in good agreement.

**Keywords** Corrosion inhibition · AFM · Kinetic parameters · Thermodynamic parameters · EIS

## 1 Introduction

Metals and alloys are used in different developmental activities and are susceptible to corrosion due to their thermodynamic instability especially in aggressive media. Corrosion is a thermodynamically feasible process because it is associated with negative change of the Gibbs free

energy. The use of inhibitors is one of the most practical methods to protect metals against acid attack. Organic substances have been used extensively as corrosion inhibitors during the last four decades. Of these, heterocyclic compounds containing one or more N, O, and S atoms can affect the inhibition of corrosion of metals in aqueous acid solution [1–8]. Among different hetero atom containing compounds, condensation products of isatin have been reported to be a potential inhibitor for different metals. This behavior of isatin derivatives has opened a new avenue for exploring the applicability of such compounds as corrosion inhibitors for mild steel in aqueous HCl solutions. Under certain conditions, the electronic structure of the organic inhibitors has a key influence on the corrosion inhibition efficiency to the metal. The inhibitors influence the kinetics of the electrochemical reactions which constitute the corrosion process and thereby modify the metal dissolution in acids. The existing data show that most organic inhibitors act by adsorption on the metal surface. They change the structure of the electrical double layer by adsorption on the metal surface. Quite a number of studies have been carried out in determination of adsorptivity of various compounds at the electrode/solution interface [9–12]. The type of interaction of inhibitor on the electrode surface during corrosion has been deduced from its adsorption characteristics by several authors [13–16].

Inspection of literature revealed that few Mannich bases have been reported effective acidic [17, 18] and vapor phase corrosion inhibitors [19]. In view of appreciable efficiency of Mannich bases, a series of new Mannich bases namely, [N-(Morpholinomethyl)-isatin-3-thiocarbohydrazone] (MOH), [N-(Morpholinomethyl)-5-nitroisatin-3-thiocarbohydrazone] (5-NMOH), and [N-(Morpholinomethyl)-5-bromoisatin-3-thiocarbohydrazone] (5-BMOH) have been synthesized to investigate its inhibition activities on corrosion of mild steel

A. K. Singh · M. A. Quraishi (✉)  
Department of Applied Chemistry, Institute of Technology,  
Banaras Hindu University, Varanasi 221 005, India  
e-mail: maquraishi@rediffmail.com;  
maquraishi.apc@itbhu.ac.in

in aqueous HCl solution using weight loss, polarization resistance, Tafel polarization, electrochemical impedance (EIS), and atomic force microscopy (AFM) techniques. The effects of temperature and immersion time were also studied.

## 2 Experimental

### 2.1 Materials

Mild steel strips composed of (wt%) C = 0.17, Mn = 0.46, Si = 0.26, S = 0.017, p = 0.019 and balance Fe were pre-treated prior to the experiment by grinding with emery paper (grade 600, 800, 1000 and 1200) then cleaned with double-distilled water, degreased with acetone and dried. The rectangular specimens with dimension 2.5 × 2.0 × 0.025 cm were used in weight loss experiments and of size 1.0 cm × 1.0 cm (exposed) with a 7.5-cm long stem (isolated with commercially available lacquer) were used for electrochemical measurements. The solutions (1 M HCl) were prepared by dilution of an analytical grade HCl with double-distilled water.

### 2.2 Inhibitors

Isatins and thiocarbohydrazide (1:1 M ratio) were refluxed in ethanol for 2–3 h, cooled and the precipitate was filtered. This product was subsequently treated with formaldehyde and morpholine to get the desired product [20, 21]. The name and molecular structure of studied compounds were given as Scheme 1.

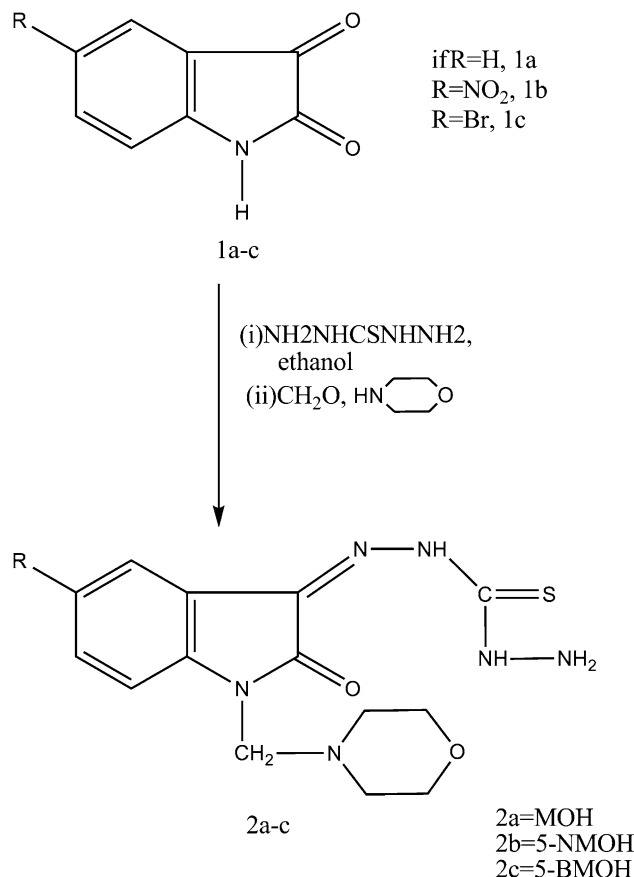
### 2.3 Weight loss studies

Weight loss experiments were done according to the method described previously [22, 23]. Weight loss measurements were performed at 308 K (except for temperature effect) for 3 h (except for immersion time effect) by immersing the mild steel coupons into acid solution (100 mL) without and with various amounts of inhibitors. After the elapsed time, the specimen were taken out, washed, dried, and weighed accurately. All the tests were conducted in aerated 1 M HCl. All the experiments were performed in triplicate and average values were reported. All the concentrations of inhibitors for weight loss and electrochemical study were taken in ppm.

The surface coverage ( $\theta$ ) and inhibition efficiency ( $\mu_{WL\%}$ ) were determined by using following equations:

$$\theta = \frac{w_o - w_i}{w_o} \quad (1)$$

$$\mu_{WL\%} = \frac{w_o - w_i}{w_o} \times 100 \quad (2)$$



**Scheme 1** Structure and synthetic route of Mannich bases

where,  $w_i$  and  $w_o$  are the weight loss value in presence and absence of inhibitors, respectively.

### 2.4 Electrochemical measurements

All electrochemical experiments were performed in Gamry electrochemical cell with three electrodes connected to Gamry Instrument Potentiostat/Galvanostat with a Gamry framework system based on ESA400. Gamry applications include software DC105 for corrosion and EIS300 for EIS measurements, and Echem Analyst version 5.50 software packages for data fitting. The mild steel of 1 cm<sup>2</sup> was the working electrode, platinum electrode was used as an auxiliary electrode, and standard calomel electrode (SCE) was used as reference electrode. All potentials were measured versus SCE.

Tafel curves were obtained by changing the electrode potential automatically from –250 to +250 mV versus corrosion potential ( $E_{corr}$ ) at a scan rate of 1 mV s<sup>–1</sup>. EIS measurements were carried out in a frequency range from 100 to 10 MHz under potentiodynamic conditions, with amplitude of 10 mV peak-to-peak, using AC signal at  $E_{corr}$ . All experiments were measured after immersion for 30 min in 1.0 M HCl with and without addition of inhibitors.

The linear polarization study was carried out from cathodic potential of  $-20$  mV versus OCP to an anodic potential of  $+20$  mV versus OCP with a scan rate  $0.125$  mV s $^{-1}$  to study the polarization resistance ( $R_p$ ).

## 2.5 Atomic force microscopy

The mild steel strips of  $1.0\text{ cm} \times 1.0\text{ cm} \times 0.025\text{ cm}$  sizes were prepared as described in Sect. 2.4. After immersion in  $1.0\text{ M HCl}$  with and without addition of  $200$  ppm of all the three Mannich bases at  $308\text{ K}$  for  $3\text{ h}$ , the specimen were cleaned with distilled water, dried, and then used for AFM.

## 3 Result and discussion

### 3.1 Weight loss studies

#### 3.1.1 Effect of inhibitor concentration

The corrosion rate decreased considerably with an increase in concentration of each inhibitor and reached the minimum value in the range of  $200\text{--}250$  ppm concentrations. The optimum concentration of inhibitors was evaluated based on their inhibition efficiency. All the synthesized compounds inhibit the corrosion. It is obvious that inhibition efficiency values for the three tested Mannich bases increase with the increase in inhibitor concentration, and this increase in the inhibition efficiency, at a given inhibitor concentration, enhances in the following order:  $5\text{-NMOH} < MOH < 5\text{-BMOH}$ . The inhibition action of Mannich bases can be explained by considering the following mechanism:  $Fe\text{ (Inh)}_{ads}$ , reaction intermediates [24]:  $Fe + Inh \leftrightarrow Fe\text{ (Inh)}_{ads} \leftrightarrow Fe^{n+} + ne^- + Inh$ . At first, when there is not enough  $Fe\text{(Inh)}_{ads}$  to cover the metal surface, because the inhibitor concentration is low or because the adsorption rate is slow, metal dissolution takes place in sites on the mild steel surface free of  $Fe\text{(Inh)}_{ads}$ . With high inhibitor concentration, a compact and coherent inhibitor over film is formed on the mild steel which reduces chemical attacks on the metal.

#### 3.1.2 Effect of immersion time

The variation of inhibition efficiency of all the three Mannich bases with immersion time is shown in Fig. 1. The inhibition efficiency of the inhibitors was found to increase with time up to  $12\text{ h}$  and thereafter remains almost constant, suggesting the formation of persistent film on the metal surface.

#### 3.1.3 Effect of temperature

In order to study the effect of temperature on the inhibition characteristic of all the Mannich bases, weight loss

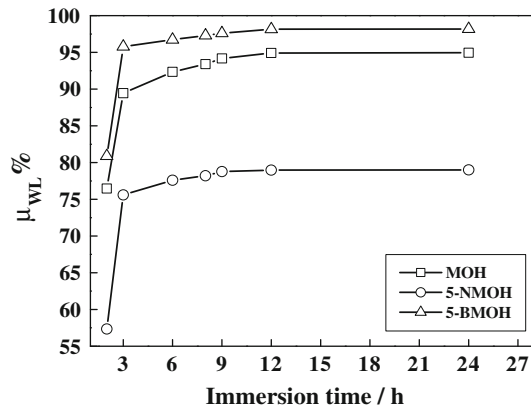


**Fig. 1** Variation of inhibition efficiency with different immersion time in  $1\text{ M HCl}$  on mild steel of surface area  $10\text{ cm}^2$  at  $200\text{ ppm}$  concentration of Mannich bases

measurements were performed at different temperatures from  $308$  to  $338\text{ K}$  in the absence and presence of different concentrations of all Mannich bases for  $3\text{ h}$  immersion time and the effect of temperature on corrosion rate at different inhibitor concentration is shown in Fig. 2.

As detected from Fig. 2, corrosion rate decreased in the presence of optimum concentration of MOH, 5-BMOH, and 5-NMOH in studied temperature range. This behavior suggests that a protective film of these compounds was formed on the mild steel surface. The effect of temperature on inhibition efficiency of these compounds indicated that the protective layer formed on the mild steel surface is comparatively less stable in the case of 5-NMOH than MOH and 5-BMOH. In the case of 5-NMOH, nitro group tend to withdraw electron density from aromatic ring hence, availability of  $\pi$ -electrons of aromatic ring is decreased to some extent. Thus, the co-ordination ability of 5-NMOH with mild steel is affected at higher temperature.

The dependence of corrosion rate at temperature can be expressed by Arrhenius equation and transition state equation [25, 26]:

$$\log(CR) = \frac{-E_a}{2.303RT} + \log \lambda \quad (3)$$

$$CR = \frac{RT}{Nh} \exp\left(\frac{\Delta S_a^*}{R}\right) \exp\left(-\frac{\Delta H_a^*}{RT}\right) \quad (4)$$

where  $E_a$  apparent activation energy,  $\lambda$  the pre-exponential factor,  $\Delta H_a^*$  the apparent enthalpy of activation,  $\Delta S_a^*$  the apparent entropy of activation,  $h$  Planck's constant and  $N$  the Avogadro number, respectively.

The apparent activation energy and pre-exponential factors for a wide range of concentration of Mannich bases can be calculated by linear regression between  $\log CR$  and  $1/T$ , the results were shown in Table 1. All the linear regression coefficients are close to 1, indicating that corrosion of mild steel in hydrochloric acid can be explained

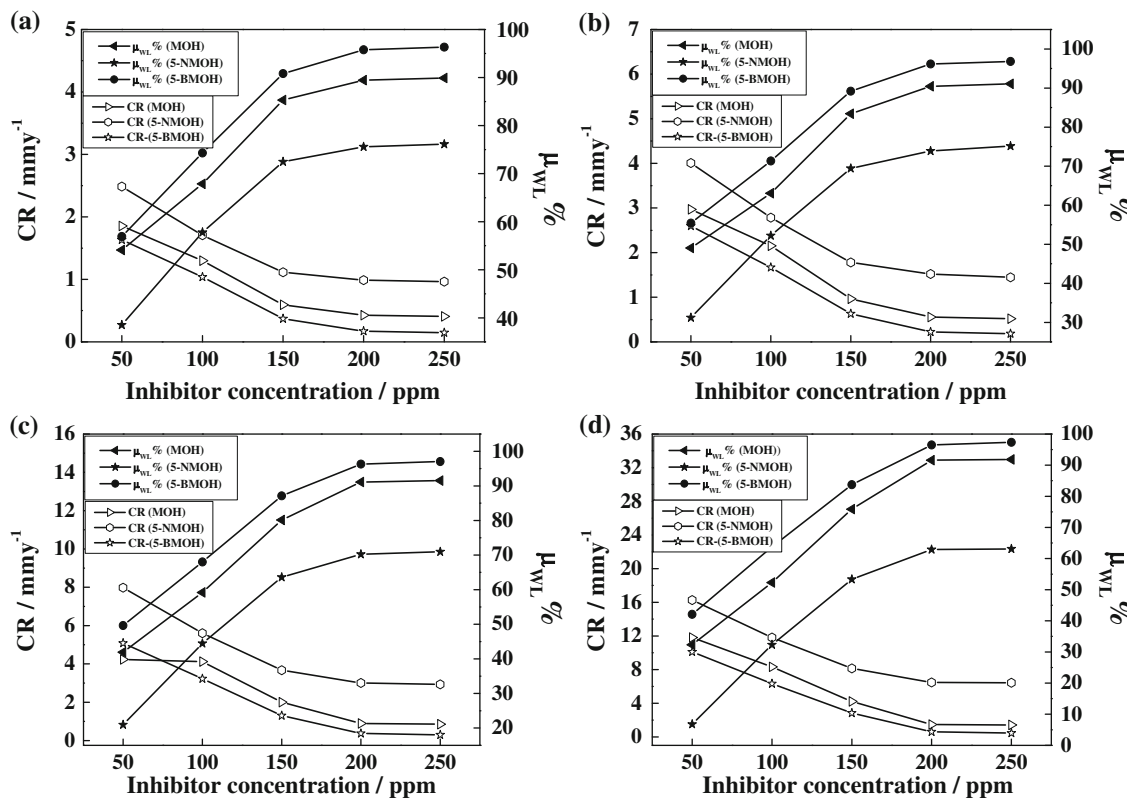


**Fig. 2** Variation of corrosion rate and inhibition efficiency in absence and presence of different concentrations of different Mannich bases in 1 M HCl on mild steel of surface area 10 cm<sup>2</sup> for 3 h immersion time at **a** 308 K, **b** 318 K, **c** 328 K and **d** 338 K

using the kinetic model. Figure 3 depicted an Arrhenius plots for mild steel immersed in 1 M HCl in presence of different concentration of isatin derivatives. The plots obtained are straight lines and the slope of each straight line gives its apparent activation energy. Table 1 summarizes  $E_a$  values for a wide range of concentration of the three molecules tested. Inspection of Table 1 showed that at lower concentration of all the inhibitor, activation energy increased compared to the free acid solution. The increase in  $E_a$  could be interpreted as the physical adsorption which occurs in the first stage [27–33]. Unchanged or lowered energy is related to the existence of chemisorption. However, it is known that mixed adsorption should be characterized by minor or no changes in activation energy. Upward or downward changes might express the advantageous physical or chemical bonding [34]. From the Table 1, it can be seen that for a wide range of inhibitor concentrations,  $E_a$  is higher for inhibited solution than free acid solution (42.21 kJ mol<sup>-1</sup>). At highest concentration, activation energy was found to decrease and these data agree with that reported in literature [33, 35]. The increase in activation energy can be attributed to an appreciable decrease in the adsorption of the inhibitor on the surface of mild steel with increasing temperature.

The results obtained in the study could be explained by the mechanism proposed by Riggs and Hurd [34]. The authors suggested that the corrosion rate,  $-d(Fe)/dt$ , can be expressed by sum of two rates:  $-d(Fe)/dt = k_1(1 - \theta) + k_2\theta$ , where  $k_1$  and  $k_2$  are the rate constants for the uninhibited reaction and completely covered surface, respectively, and  $\theta$  is the fraction of surface covered by adsorbed inhibitor.

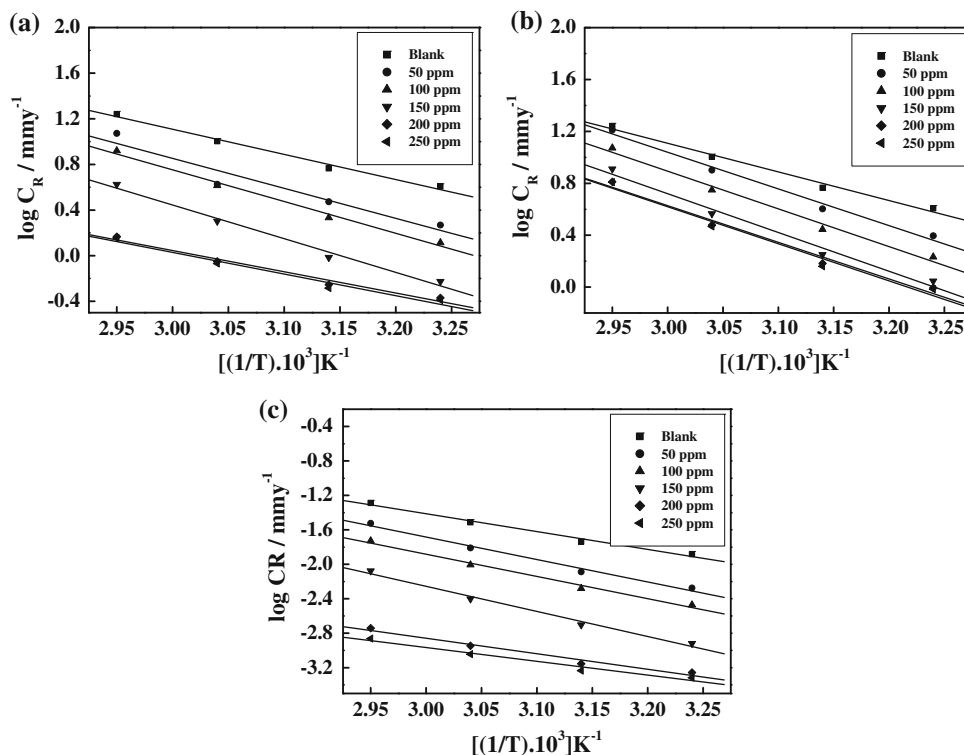
The Fe (Inh)<sub>ads</sub>, reaction intermediates [24]:  $Fe + Inh \leftrightarrow Fe^- (Inh)_{ads} + Fe^{n+} + ne^- + Inh$  can explain the inhibition mechanism. At first, when there is not enough Fe (Inh)<sub>ads</sub> to cover the metal surface, because the inhibitor concentration is low or because the adsorption rate is slow, metal dissolution takes place on the mild steel surface free of Fe (Inh)<sub>ads</sub>. With high inhibitor concentration, a compact and coherent inhibitor over film is formed on the mild steel which reduces chemical attacks on the metal.

In many systems,  $k_2$  may be so small that  $k_2\theta$  may be negligible. When  $\theta$  becomes quite large ( $>0.9$ ), very small increase in  $k_2$  causes the term  $k_1(1 - \theta)$  to decrease markedly so that it would take a very large ratio of  $k_1/k_2$  to make the term  $k_2\theta$  negligible at high coverage. Thus, the corrosion rates of many inhibited systems at high coverage do no suggest simply the high degree of adsorption but

**Table 1** Thermodynamic activation parameters for mild steel in 1 M HCl in absence and presence of different concentrations of different inhibitors

Name of inhibitor	Concentration of inhibitor (ppm)	$E_a$ (kJ mol <sup>-1</sup> )	$\lambda$ (mg cm <sup>-2</sup> )	$\Delta H^*$ (kJ mol <sup>-1</sup> )	$\Delta S^*$ (J mol <sup>-1</sup> K <sup>-1</sup> )
1 M HCl	0	42.21	$5.31 \times 10^8$	39.57	-86.75
MOH	50	50.28	$5.43 \times 10^8$	47.63	-87.57
	100	53.22	$1.24 \times 10^9$	50.56	-79.66
	150	56.49	$1.99 \times 10^9$	53.84	-75.74
	200	35.63	$4.28 \times 10^5$	32.98	-145.96
	250	36.33	$5.29 \times 10^5$	33.67	-144.18
	5-NMOH	54.07	$3.27 \times 10^9$	51.41	-71.63
5-NMOH	100	55.60	$4.06 \times 10^9$	52.94	-69.83
	150	57.19	$4.84 \times 10^9$	54.54	-68.37
	200	54.01	$1.24 \times 10^9$	51.36	-79.67
	250	54.65	$1.53 \times 10^9$	52.00	-77.91
5-BMOH	50	52.51	$1.17 \times 10^9$	49.85	-80.15
	100	58.35	$2.59 \times 10^9$	51.24	-76.00
	150	51.98	$6.12 \times 10^8$	55.70	-73.58
	200	35.10	$3.02 \times 10^5$	34.45	-148.86
	250	35.52	$4.79 \times 10^5$	34.56	-147.67

**Fig. 3** Adsorption isotherm plots for log CR versus 1/T at different concentrations of **a** MOH, **b** 5-NMOH and **c** 5-BMOH

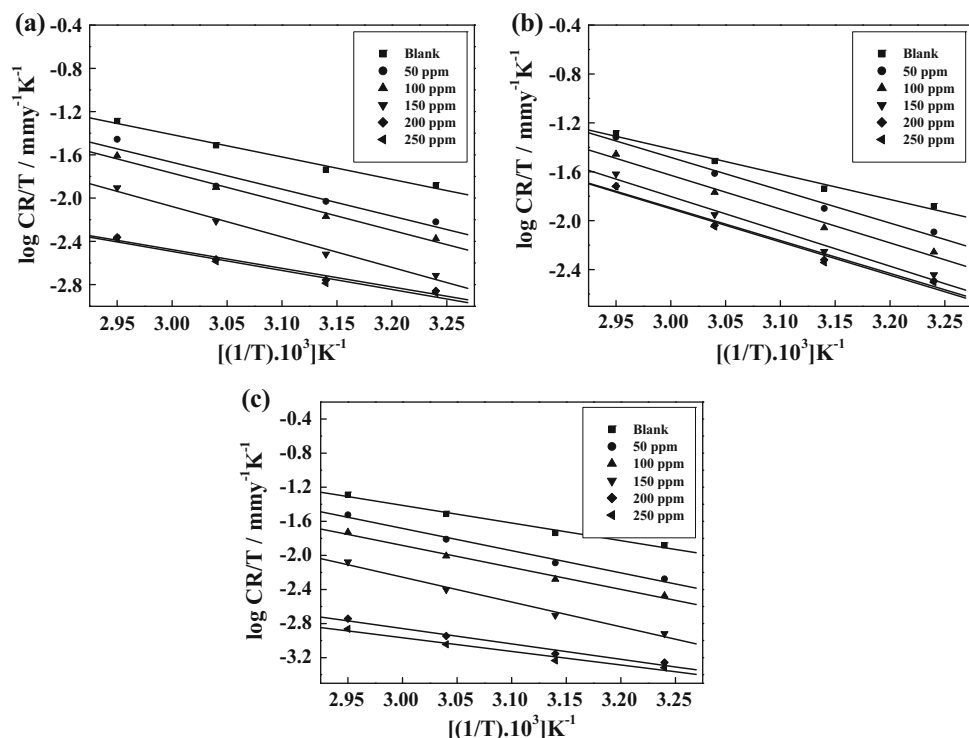


rather a new expression, i.e., simply  $k_2\theta$ . In such cases, the term  $k_1(1-\theta)$  will be negligible and the corrosion mechanism probably involves direct reaction of the species “metal atom-adsorbed inhibitor molecules”. It is, thus, probable that the activation energy in  $k_2 = \lambda e^{-\Delta E_2/RT}$  will be quite different from that in the uninhibited rate constant  $k_1$ . Thus, it is possible that the activation energy of inhibited reaction at high coverage can be either larger or

smaller than that of the uninhibited reaction. The trend of activation energies in the present study may be followed in this way.

The relationship between  $\log(CR/T)$  and  $1/T$  was shown in Fig. 4. Straight lines are obtained with a slope  $(-\Delta H_a^*/2.303R)$  and an intercept of  $[\log(R/Nh) + (\Delta S_a^*/2.303R)]$ , from which the value of  $\Delta H_a^*$  and  $\Delta S_a^*$  were calculated and presented in Table 1.

**Fig. 4** Adsorption isotherm plots for  $\log(CR/T)$  versus  $1/T$  at different concentrations of **a** MOH, **b** 5-NMOH and **c** 5-BMOH



The relationship between activation energy and enthalpy of activation against the concentration of all the Mannich bases is shown in Fig. 5. From the data obtained in Table 1, it is clear that  $E_a$ ,  $\Delta H_a^*$  vary in the same manner in the case of MOH, 5-NMOH, and 5-BMOH. However, the variation in the case of 5-NMOH is different from MOH and 5-BMOH. In the case of 5-NMOH, in all the concentration range, activation parameters are almost constant, whereas in the other two cases, activation parameters increase first, reaches maximum and thereafter gradually decrease. In the case of MOH and 5-BMOH, this phenomenon is interpreted by the fact that at a relatively lower concentration, the

reduction in mild steel corrosion rate is mainly decided by kinetic parameters of activation. When the concentration is relatively increased, the decrease in mild steel corrosion rate is chiefly controlled by pre-exponential factor and in the case of 5-NMOH, there was no dramatic change in the value of A, and, therefore, the decrease in corrosion rate is mainly controlled by activation energy [36].

On comparing the values of entropy of activation ( $\Delta S_a^*$ ) listed in Table 1, it is clear that entropy of activation decreased in presence of MOH, 5-NMOH, and 5-BMOH compared to free acid solution. Such variation is associated with the phenomenon of ordering and disordering of inhibitor molecules on the mild steel surface. The decrease of entropy of activation in the presence of MOH, 5-NMOH, and 5-BMOH reflects the formation of an ordered stable film of inhibitor on the mild steel surface [26, 37]. Investigation of Table 1 reveals that the change in randomness is comparatively smaller than MOH and 5-BMOH ongoing from reactant to activated complex [38–40].

### 3.2 Thermodynamic parameters and adsorption isotherm

The adsorption on the corroding surfaces never reaches the real equilibrium and tends to reach an adsorption steady state. When corrosion rate is sufficiently decreased in the presence of inhibitor, the adsorption steady state has a tendency to attain quasi-equilibrium state. Now, it is reasonable to consider quasi-equilibrium adsorption in

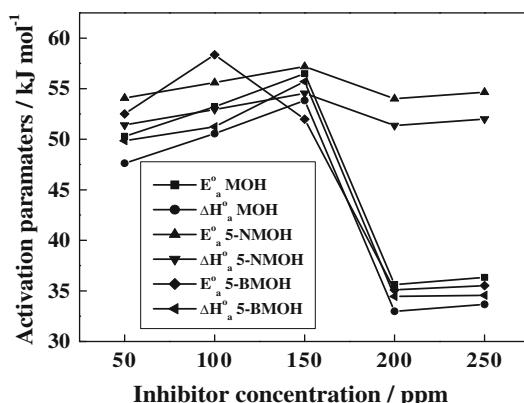


**Fig. 5** Variation of kinetic parameters with different concentrations of different Mannich bases

thermodynamic way using the appropriate adsorption isotherm. The degree of surface coverage ( $\theta$ ) for inhibitor was obtained from average weight loss data. Langmuir, Temkin, and Frumkin adsorption isotherms were tested to find the best suitable adsorption isotherm for adsorption of Mannich bases on the surface of mild steel from 1.0 M HCl solution. Langmuir adsorption isotherm (Eq. 5) was found fit. With regard to the Langmuir adsorption isotherm, the surface coverage ( $\theta$ ) of the inhibitor on the mild steel surface is related to the concentration ( $C_{\text{inh}}$ ) of the inhibitor in the bulk of the solution according to the following equation:

$$\theta = \frac{K_{\text{ads}} C_{\text{inh}}}{1 + K_{\text{ads}} C_{\text{inh}}} \quad (5)$$

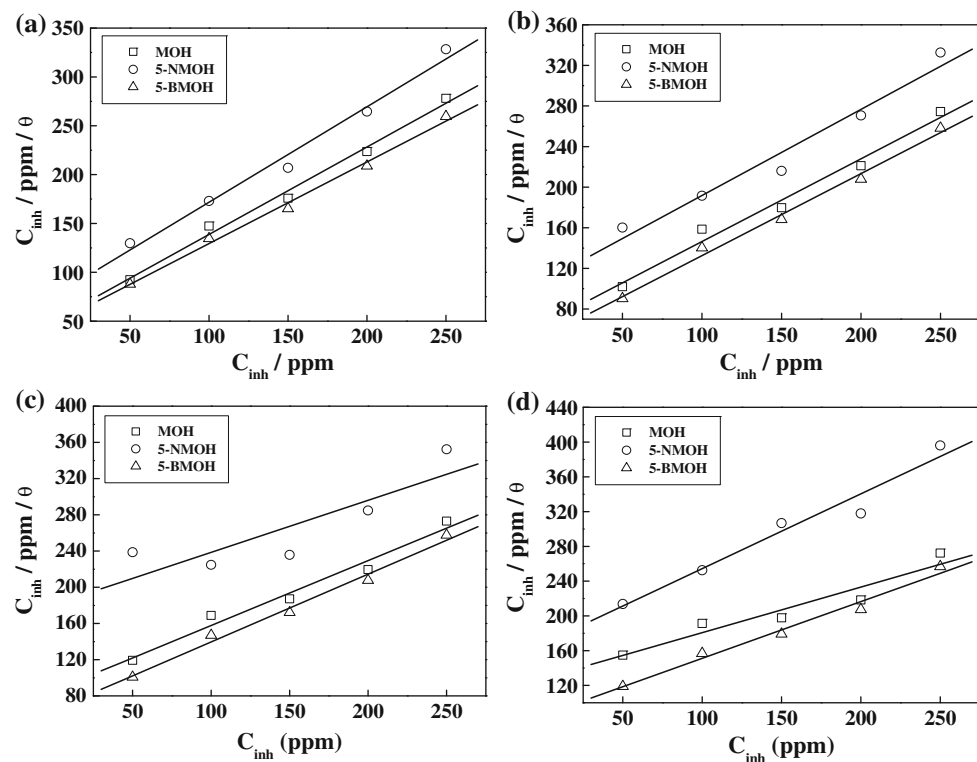
where,  $K_{\text{ads}}$  is the equilibrium constant for the adsorption/desorption process. This equation can be rearranged to

$$\frac{C_{\text{inh}}}{\theta} = \frac{1}{K_{\text{ads}}} + C_{\text{inh}} \quad (6)$$

It is known fact that  $K_{\text{ads}}$  represents the strength between adsorbate and adsorbent. Large values of  $K_{\text{ads}}$  imply more efficient adsorption and hence better inhibition efficiency [41].

From the intercepts of the straight lines on the  $C/\theta$ -axis (Fig. 6),  $K_{\text{ads}}$  can be calculated which is related to free energy of adsorption,  $\Delta G_{\text{ads}}^{\circ}$ , as given by Eq. 7.

**Fig. 6** Langmuir's adsorption isotherm plots for the adsorption of Mannich bases in 1 M HCl on the surface of mild steel at **a** 308 K, **b** 318 K, **c** 328 K and **d** 338 K



$$\Delta G_{\text{ads}}^{\circ} = -RT \ln(55.5K_{\text{ads}}) \quad (7)$$

The negative values of  $\Delta G_{\text{ads}}^{\circ}$  ensure the spontaneity of the adsorption process and stability of the adsorbed layer on the mild steel surface [42, 43]. It is usually accepted that the value of  $\Delta G_{\text{ads}}^{\circ}$  around  $-20 \text{ kJ mol}^{-1}$  or lower indicates the electrostatic interaction between charged metal surface and charged organic molecules in the bulk of the solution while those around  $-40 \text{ kJ mol}^{-1}$  or higher involve charge sharing or charge transfer between the metal surface and organic molecules [44].

Assuming thermodynamic model, corrosion inhibition of mild steel in the presence of Mannich bases can be better explained, therefore, heat of adsorption and entropy of adsorption were calculated.

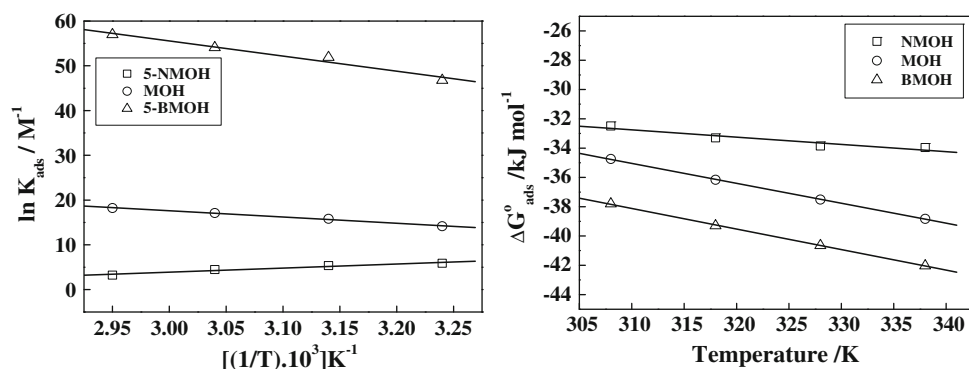
According to Van't Hoff equation [45]:

$$\ln K_{\text{ads}} = (-\Delta H_{\text{ads}}^{\circ}/RT) + \text{constant} \quad (8)$$

In order to calculate adsorption heat,  $\ln K_{\text{ads}}$  was plotted against  $1/T$ , as shown in Fig. 7a. The straight lines were obtained with slope equal to  $(-\Delta H_{\text{ads}}^{\circ}/R)$  and intercept equal to  $(\Delta S_{\text{ads}}^{\circ}/R + \ln 1/55.5)$ . The calculated values of heat of adsorption and entropy of adsorption are listed in Table 2. Under the experimental conditions, the adsorption heat could be approximately regarded as the standard adsorption heat ( $\Delta H_{\text{ads}}^{\circ}$ ).

The thermodynamic parameters  $\Delta H_{\text{ads}}^{\circ}$  and  $\Delta S_{\text{ads}}^{\circ}$  can also be calculated from the following equation:

**Fig. 7** Adsorption isotherm plot for **a**  $\ln K_{\text{ads}}$  versus  $1/T$  and **b**  $\Delta G_{\text{ads}}^{\circ}$  versus  $T$  for adsorption of different Mannich bases on mild steel in 1 M HCl



$$\Delta G_{\text{ads}}^{\circ} = \Delta H_{\text{ads}}^{\circ} - T \Delta S_{\text{ads}}^{\circ} \quad (9)$$

A plot of  $\Delta G_{\text{ads}}^{\circ}$  versus  $T$  gives straight lines (Fig. 7b) with the slope equal to  $-\Delta S_{\text{ads}}^{\circ}$ , and the value of  $\Delta H_{\text{ads}}^{\circ}$  can be calculated from intercept. Values of  $\Delta H_{\text{ads}}^{\circ}$  and  $\Delta S_{\text{ads}}^{\circ}$  obtained by both methods follow the same trend.

The sign of enthalpy of adsorption is negative in the case of MOH, whereas positive in 5-NMOH and 5-BMOH. The values of entropy of adsorption are positive in all the cases. In fact, it is well known fact that adsorption is an exothermic phenomenon accompanied by a decrease in entropy [46]. In aqueous solution, the adsorption of organic molecule is generally accompanied with desorption of water molecules. The adsorption of an organic adsorbate at the metal/solution interface is considered a “substitutional adsorption” phenomenon [47]. Therefore, the positive values of  $\Delta H_{\text{ads}}^{\circ}$  and  $\Delta S_{\text{ads}}^{\circ}$  related to “substitutional adsorption” can be attributed to the increase in the solvent entropy and to a more positive water desorption enthalpy. Inspection of Table 2 revealed that decrease in enthalpy is the driving force for the adsorption of MOH, whereas

increase in entropy is the driving force for the adsorption of 5-NMOH and 5-BMOH on the mild steel surface.

### 3.3 Electrochemical impedance spectroscopy

Electrochemical impedance measurements were carried out over the frequency range from 100 to 0.01 Hz at open circuit potential. The appropriate circuit for studies was shown in Fig. 8. Nyquist plots of mild steel having various concentrations of all the Mannich bases in 1.0 M HCl solutions are given in Fig. 9a–c. Inhibition efficiency can be calculated from Nyquist plot as follows:

$$\mu_{R_{\text{ct}}\%} = \frac{R_{\text{ct}}^{\text{i}} - R_{\text{ct}}^{\text{o}}}{R_{\text{ct}}^{\text{i}}} \times 100 \quad (10)$$

where,  $R_{\text{ct}}^{\text{i}}$  and  $R_{\text{ct}}^{\text{o}}$  are the charge transfer resistance of mild steel with and without inhibitor molecules, respectively. Inhibition efficiencies and other calculated impedance parameters are presented in Table 3.

The impedance response of mild steel in acid solution was significantly changed after the addition of all the

**Table 2** Thermodynamic parameters for the adsorption of inhibitors in 1 M HCl on the mild steel at different temperatures

Name of inhibitor	Temperature (K)	$K_{\text{ads}} (10^3 \text{ M}^{-1})$	$-\Delta G_{\text{ads}}^{\circ} (\text{kJ mol}^{-1})$	$\Delta H_{\text{ads}}^{\circ} (\text{kJ mol}^{-1})$	$\Delta S_{\text{ads}}^{\circ} (\text{J mol}^{-1} \text{ K}^{-1})$	$\Delta H_{\text{ads}}^{\circ \text{ a}} (\text{kJ mol}^{-1})$	$\Delta S_{\text{ads}}^{\circ \text{ a}} (\text{J mol}^{-1} \text{ K}^{-1})$
MOH	308	14.15	34.74	-16.90	57.92	-17.37	49.60
	318	15.80	36.16	-16.90	60.56	-	-
	328	17.12	37.51	-16.90	62.83	-	-
	338	18.21	38.83	-16.90	64.88	-	-
5-NMOH	308	5.88	32.49	7.19	128.83	7.18	134.20
	318	5.36	33.30	7.19	127.32	-	-
	328	4.47	33.85	7.19	125.12	-	-
	338	3.21	33.96	7.19	121.74	-	-
5-BMOH	308	46.78	37.80	5.43	140.35	5.40	140.40
	318	51.88	39.30	5.43	140.66	-	-
	328	54.08	40.65	5.43	140.48	-	-
	338	56.97	42.03	5.43	140.41	-	-

<sup>a</sup> Calculated using Eq. 9

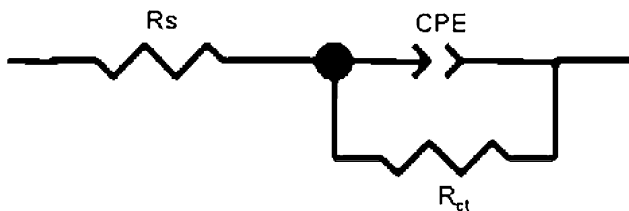


**Fig. 8** Electrochemical equivalent circuit used to fit the impedance spectra

Mannich bases, and the impedance of the inhibited system increased with inhibitor concentration. Furthermore, at 200 ppm concentration of Mannich bases gives rise to much larger semicircle diameter than other two lower concentrations of Mannich bases (Fig. 9a–c). In the presence of all the Mannich bases, in the completely studied concentration interval, the electrochemical impedance spectra in complex plane presentation (Nyquist diagram) are characterized by one depressed semicircle, with a high frequency capacitive loop and low frequency inductive loop. Deviation from perfect circular shape, often known as frequency dispersion, was attributed to surface roughness and inhomogeneities of the solid surface [48, 49]. The high frequency capacitive loop may be due to a charge transfer process. In the presence of lower concentration of MOH and 5-BMOH and all the concentration of 5-NMOH, the low frequency inductive loop can be attributed to bulk relaxation process of the adsorbed compound or to a

dissolution process [50]. It might be also attributed to the re-dissolution of the passivated surface at low frequencies. The fact that this semicircle cannot be observed after the addition of higher concentration of MOH and 5-BMOH supports our view.

In order to get more accurate fit of these experimental data, constant phase element has used instead of capacitive element. The CPE impedance is given by [51]:

$$Z_{\text{CPE}} = Y_0^{-1} (i\omega)^{-n} \quad (11)$$

where  $Y_0$  is the CPE constant,  $\omega$  is the angular frequency (in  $\text{rad s}^{-1}$ ),  $i^2 = -1$  is the imaginary number and  $n$  is a CPE exponent which can be used as a gauge of the heterogeneity or roughness of the surface [52]. Depending on the value of  $n$ , CPE can represent resistance ( $n = 0$ ,  $Y_0 = R$ ), capacitance ( $n = 1$ ,  $Y_0 = C$ ), inductance ( $n = -1$ ,  $Y_0 = L$ ) or Warburg impedance ( $n = 0.5$ ,  $Y_0 = W$ ).

The electrochemical parameters, including  $R_s$ ,  $R_{\text{ct}}$ ,  $Y_0$ , and  $n$ , obtained from fitting the recorded EIS data using the equivalent circuit of Fig. 8, were listed in Table 3.  $C_{\text{dl}}$  values derived from CPE parameters according to Eq. 12 were also listed in Table 3.

$$C_{\text{dl}} = (Y_0 \cdot R_{\text{ct}}^{1-n})^{1/n} \quad (12)$$

Inspection of the results in Table 3 indicated that the  $R_{\text{ct}}$  value increased with the concentration of Mannich bases. In addition, the value of the proportional factor  $Y_0$  of CPE varies in a regular manner with inhibitor concentration.

**Fig. 9** Nyquist plots of mild steel in 1 M HCl with different concentrations of **a** MOH, **b** 5-NMOH, and **c** 5-BMOH

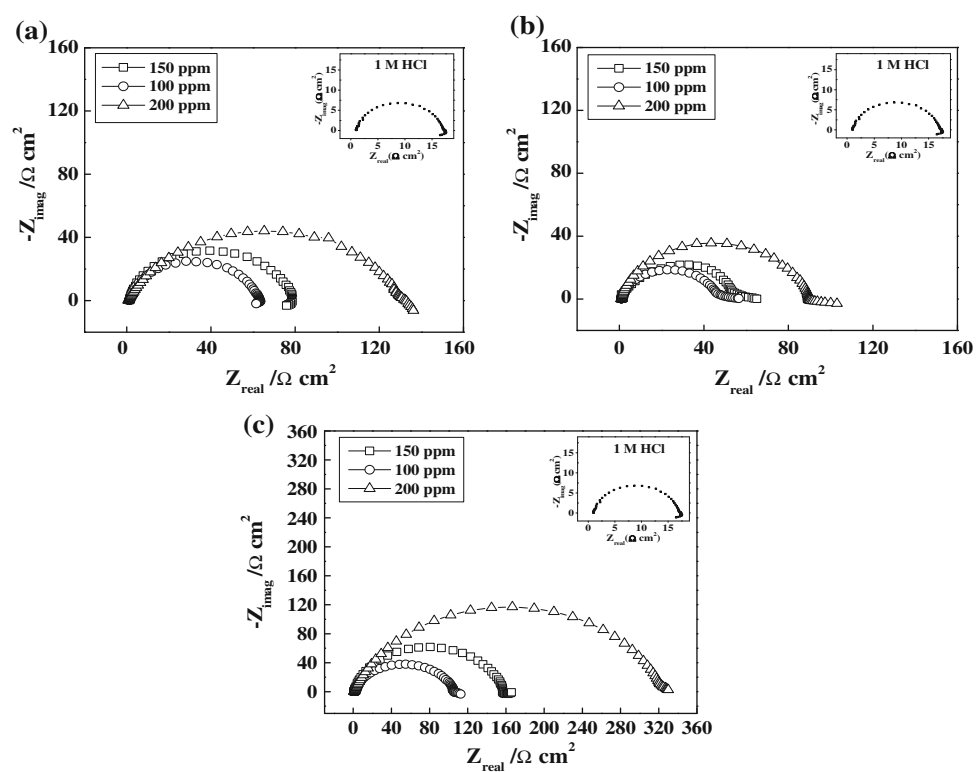


**Table 3** Impedance parameters and inhibition efficiency values for mild steel after 30 min immersion period in 1 M HCl in absence and presence of different concentrations of different inhibitors

Name of inhibitor	Concentration of inhibitor (ppm)	$R_s$ ( $\Omega \text{ cm}^2$ )	$R_{ct}$ ( $\Omega \text{ cm}^2$ )	$Y_o$ ( $\mu\text{F cm}^{-2}$ )	$n$	$C_{dl}$ ( $\mu\text{F cm}^{-2}$ )	$\mu_{R_{ct}}\%$
1 M HCl	0	1.32	17.24	162.0	0.845	55.09	—
MOH	100	1.12	63.34	197.1	0.759	49.00	72.78
	150	1.24	77.82	99.7	0.852	43.08	77.84
	200	0.71	129.9	55.6	0.881	28.56	86.72
5-NMOH	100	0.87	45.99	105.9	0.868	47.12	62.51
	150	0.91	54.41	93.2	0.882	45.96	68.31
	200	0.97	90.5	72.3	0.900	41.35	80.95
5-BMOH	100	0.84	105.0	110.9	0.796	35.42	83.58
	150	0.96	154.6	80.0	0.829	32.32	88.84
	200	1.05	324.0	58.4	0.855	29.79	94.67

The change of  $R_{ct}$  and  $Y_o$  values can be related to the gradual replacement of water molecules and/or hydroxyl ions by Mannich bases molecules on the surface and consequently to a decrease in the number of active sites necessary for the corrosion reaction. The increase in  $R_{ct}$  value is attributed to the formation of protective film on the metal/solution interface. Indeed, the increase of the values of  $n$  when compared with 1 M HCl and with Mannich bases concentration can be explained by some decrease of the surface heterogeneity, due to the adsorption of the inhibitor on the most active adsorption sites [53]. Moreover, the values of double-layer capacitance,  $C_{dl}$ , decreased with increasing Mannich base concentration. The decrease in  $C_{dl}$  is probably due to a decrease in local dielectric constant and/or an increase in the thickness of a protective layer at electrode surface, enhancing, therefore, the corrosion resistance of the studied steel. The thickness of the protective layer ( $d$ ) is related to  $C_{dl}$  according to the following equation [54]:

$$C_{dl} = \frac{\epsilon \epsilon_0}{d} \quad (13)$$

where,  $\epsilon$  is the dielectric constant of the protective layer and  $\epsilon_0$  is the permittivity of free space.

It is obvious from the results that the Mannich bases inhibit the corrosion of mild steel in 1 M HCl solution at all concentrations used in this study and the  $\mu_{R_{ct}}\%$  was seen to increase continuously with increasing additive concentration at 303 K (Table 3). The inhibition efficiencies, calculated from ac impedance results, show the same trend as those obtained from weight loss measurements.

#### 3.4 Linear polarization resistance

Polarization resistance values were determined from the slope of the potential–current lines,

$$R_p = A \frac{dE}{di} \quad (14)$$

where,  $A$  is the surface area of the electrode,  $dE$  is change in potential and  $di$  is change in current. The  $R_p$  values were used to calculate the inhibition efficiencies, ( $\mu_{R_p}\%$ ) using the relationship:

$$\mu_{R_p}\% = \frac{R_p^i - R_p^0}{R_p^i} \times 100 \quad (15)$$

where,  $R_p^i$ , and  $R_p^0$  are the polarization resistances in the presence and absence of inhibitor, respectively. The inhibition efficiencies and polarization resistance parameters are presented in Table 4.

#### 3.5 Tafel polarization

The values of corrosion potential ( $E_{corr}$ ), corrosion current density ( $i_{corr}$ ), and anodic and cathodic Tafel slopes ( $\beta_a$  and  $\beta_c$ ) can be evaluated from anodic and cathodic regions of Tafel plots. The linear Tafel segments of anodic and cathodic curves were extrapolated to corrosion potential to obtain corrosion current densities ( $i_{corr}$ ).

The inhibition efficiency was evaluated from the measured  $i_{corr}$  values using the relationship:

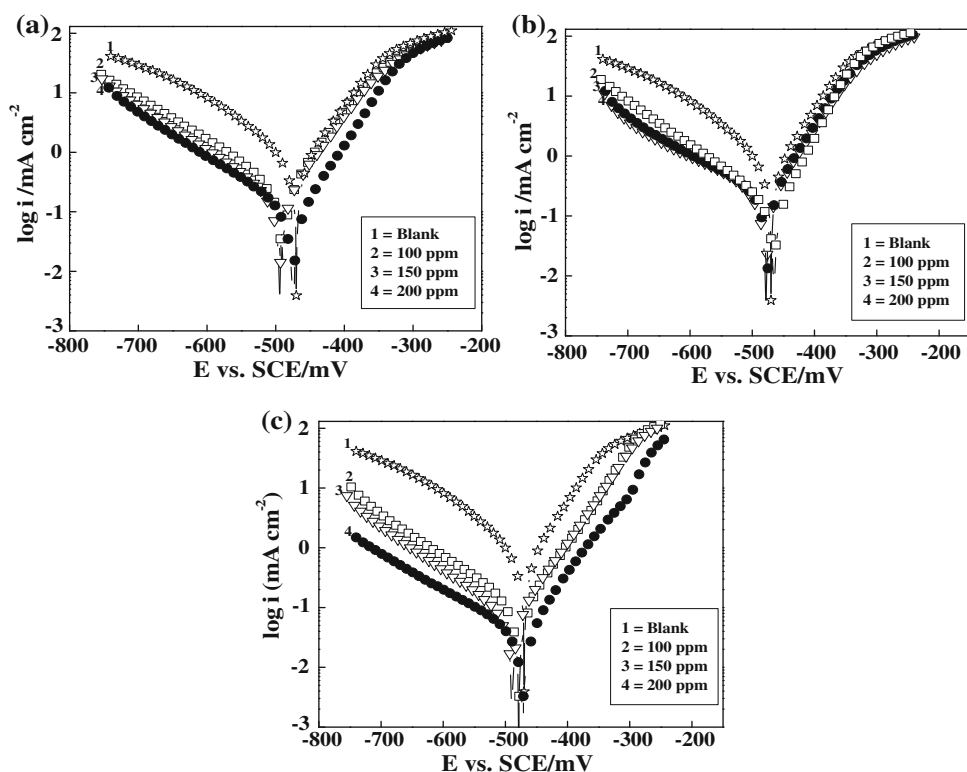
$$\mu_p\% = \frac{i_{corr}^0 - i_{corr}^i}{i_{corr}^0} \times 100 \quad (16)$$

where,  $i_{corr}^0$  and  $i_{corr}^i$  are values of corrosion current density in absence and in presence of inhibitor, respectively.

Figure 10a–c represents the potentiodynamic polarization curves of mild steel in 1 M HCl in the absence and presence of various concentrations of the MOH, 5-NMOH, and 5-BMOH. It can be seen from the Fig. 10a–c that, in the presence of inhibitor, the curves are shifted to lower current regions, showing the inhibition tendency of the

**Table 4** Potentiodynamic polarization parameters for mild steel without and with different concentrations of different inhibitors in 1 M HCl

Name of inhibitor	Concentration of inhibitor (ppm)	Linear polarization		Tafel polarization				
		$R_p$ ( $\Omega \text{ cm}^2$ )	$\mu_{R_p}\%$	$E_{\text{corr}}$ (mV vs. SCE)	$i_{\text{corr}}$ ( $\mu\text{A cm}^{-2}$ )	$\beta_a$ (mV/dec)	$\beta_c$ (mV/dec)	$\mu_p\%$
1 M HCl	0	18.69	—	−469	730.0	73	127	—
MOH	100	70.27	73.40	−490	204.0	65	107	72.05
	150	94.50	80.22	−494	179.0	72	128	75.47
	200	230.00	91.87	−474	95.0	67	115	86.98
5-NMOH	100	60.80	66.50	−477	300.0	75	257	58.90
	150	77.92	76.01	−478	239.0	74	179	67.26
	200	90.50	79.34	−465	170.0	67	140	76.71
5-BMOH	100	115.20	83.77	−478	126.0	85	160	82.73
	150	142.00	86.83	−489	92.3	84	172	87.35
	200	569.70	96.71	−472	45.0	76	213	93.83

**Fig. 10** Tafel polarization behavior of mild steel in 1 M HCl with different concentrations of **a** MOH, **b** 5-NMOH and **c** 5-BMOH

Mannich bases. There was no definite trend observed in the  $E_{\text{corr}}$  values in the presence of all the Mannich bases. In the present study, shift in  $E_{\text{corr}}$  values is in the range of 20–25 mV suggesting that they all act as mixed type of inhibitor [55, 56]. The values of various electrochemical parameters derived by Tafel polarization of all the inhibitors are given in Table 4. Investigation of Table 4 revealed that the values of  $\beta_a$  change slightly in the presence of all the Mannich bases, whereas more pronounced change occurs in the values of  $\beta_c$ , indicating that both anodic and cathodic reactions are affected but the effect on the

cathodic reactions is more prominent. Thus, all the Mannich bases acted as mixed type corrosion inhibitor, but predominantly cathodic inhibitor [57]. It is seen (Table 4) that the inhibition efficiency of all the compounds increases with the increase in the inhibitor concentration and the inhibition efficiency showed the following order: 5-NMOH < MOH < 5-BMOH. Increase in inhibition efficiencies with increasing concentration of all the three Mannich bases studied reveals that inhibition action are due to adsorption on steel surface and the adsorption is known to depend on the chemical structure of the inhibitors.

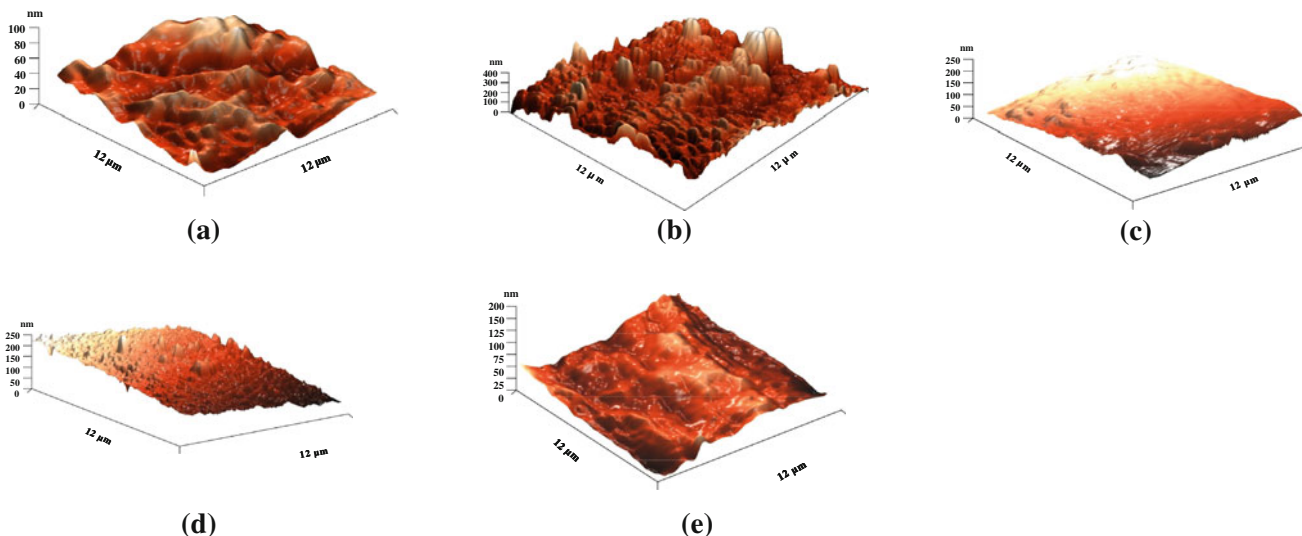


**Fig. 11** Atomic force micrographs of mild steel surface of **a** polished mild steel, **b** mild steel in 1 M HCl, **c** inhibited mild steel (1 M HCl + 200 ppm MOH), **d** inhibited mild steel (1 M HCl + 200 ppm 5-NMOH), **e** inhibited mild steel (1 M HCl + 200 ppm 5-BMOH)

The results indicate good agreement between the values of corrosion efficiency from the weight loss, polarization resistance, Tafel polarization, and impedance measurements. It is concluded that the corrosion rate depends on the chemical nature of the electrolyte rather than the applied technique [58]. The differences are sometime as high as >7–8% but the order of magnitude is the same for all the methods.

### 3.6 Surface characterization: AFM study

In order to establish whether inhibition is due to the formation of a film on the metal surface through adsorption, atomic force micrographs were taken. The three-dimensional AFM images are shown in Fig. 11a–e. As can be seen from Fig. 11c–e, there was much less damage on the surface of mild steel with all the Mannich bases. The average roughness of polished mild steel (Fig. 11a) and mild steel in 1.0 M HCl without inhibitor (Fig. 11b) was calculated to be 66 and 395 nm, respectively. The mild steel surface in the free acid solution is getting cracked due to the acid attack on the surface (Fig. 11b). However, in presence of 200 ppm concentration of all the Mannich bases, the average roughness was reduced to 220, 245, and 205 nm in the presence of MOH, 5-NMOH, and 5-BMOH, respectively (Fig. 11c–e).

## 4 Mechanism of inhibition

From the results obtained from different electrochemical and weight loss measurements, it was concluded that all the three Mannich bases (MOH, 5-NMOH, and 5-BMOH)

inhibit the corrosion of mild steel in 1 M HCl by adsorption at mild steel/solution interface (Fig. 12).

It is general assumption that the adsorption of organic inhibitors at the metal surface interface is the first step in the mechanism of the inhibitor action. Organic molecules may be adsorbed on the metal surface in four types, namely

- (i) Electrostatic interaction between the charged molecules and the charged metal,
- (ii) Interaction of unshared electron pairs in the molecule with the metal,
- (iii) Interaction of  $\pi$ -electrons with the metal and
- (iv) a combination of types (i–iii) [59–61]

In general, all the three Mannich bases, MOH, 5-NMOH, and 5-BMOH contain one iminic group ( $-\text{C}=\text{N}$ ), two secondary amino group, one primary amino group, one thio group, aromatic ring, and residue of morpholine ring.

The inhibition of active dissolution of the metal is due to the adsorption of the inhibitor molecules on the metal surface forming a protective film. The inhibitor molecules can be adsorbed onto the metal surface through electron transfer from the adsorbed species to the vacant electron orbital of low energy in the metal to form a co-ordinate type link.

The inhibition efficiency depends on many factors [62, 63] including the number of adsorption centers, mode of interactions with metal surface, molecular size, and structure.

It is well known that iron has co-ordination affinity toward nitrogen, sulfur, and oxygen-bearing ligands [64–67]. Hence, adsorption on iron can be attributed to co-ordination through iminic group, hetero atom (N and S), and  $\pi$ -electrons of aromatic ring.

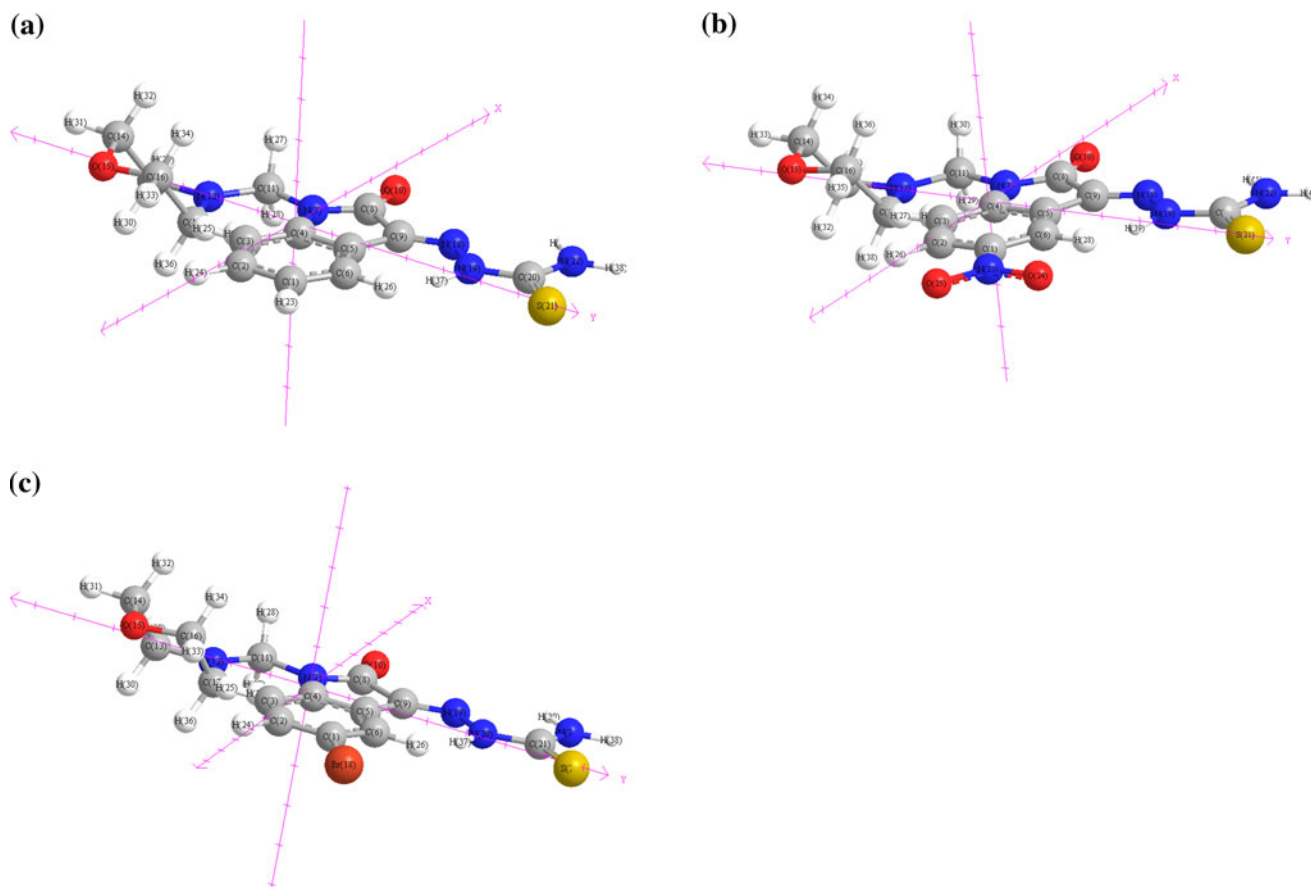


**Fig. 12** Three-dimensional representation of **a** MOH, **b** 5-NMOH and **c** 5-BMOH

If one considers the structures of investigated compounds (Scheme 1) several potential sources of inhibitor–metal interaction can be identified. In all the three Mannich bases, there are the unshared electron pairs on N and S, capable of forming a co-ordination  $\sigma$ -bond with iron [68]. Further, the double bonds in the molecule allow back donation of metal d-electrons to the  $\pi^*$ -orbital and this type of interaction cannot occur with amines. Another striking feature for high inhibition performance of all the studied compounds is the presence of S-atom. The presence of S-atom in the inhibitor structures makes the formation of  $d\pi-d\pi$  bond resulting from overlap of 3d-electrons from iron atom to the 3d vacant orbital of S-atom possible, which enhances the adsorption of the compounds on the metal surface.

The better inhibition performance of 5-BMOH than MOH is due to the presence of Br atom in its structure, because of electron releasing effect, Br increases the electron density of aromatic ring and makes the  $\pi$ -electrons more available to interact with mild steel surface. Thus, 5-BMOH is more effectively adsorbed. The difference in inhibition efficiency of MOH and 5-NMOH can be explained by considering the presence of  $\text{NO}_2$  group. The nitro group withdraws the  $\pi$ -electron density of aromatic ring and the availability of

$\pi$ -electrons for interaction with iron is decreased. Thus, 5-NMOH is not adsorbed on the mild steel surface effectively as much as MOH. Another reason for low efficiency of 5-NMOH is that due to electron withdrawing effect of nitro group, partial negative charge is developed on nitro group and due to this, there is repulsion between negatively charged mild steel surface and inhibitor molecule. Thus, the inhibition efficiency of the studied compounds follows the order 5-NMOH < MOH < 5-BMOH. The results of weight loss, EIS, linear polarization, and Tafel polarization follow the same trend.

## 5 Conclusions

All the studied Mannich bases show excellent performance as corrosion inhibitors in HCl acid solution. They inhibit corrosion of mild steel in HCl solution by an adsorption mechanism. Various measurable quantities deduced for the corrosion system with and without the inhibitor reflect the microscopic surface state of the system. The principle conclusions are

1. The adsorption of all the three Mannich bases obeyed Langmuir adsorption isotherm.
2. All the three Mannich bases acted as mixed type inhibitor.
3. The increasing value of CPE exponent ( $n$ ) with increasing inhibitor concentration indicated that surface roughness decreased with increasing inhibitor concentration.
4. The adsorption of 5MOH and 5-BMOH is favored at higher temperature while adsorption of 5-NMOH is not favored at higher temperature.
5. Decrease in enthalpy is the driving force for the adsorption of MOH while increase in entropy is the driving force for the adsorption of 5-NMOH and 5-BMOH.
6. The inhibition efficiency of tested inhibitors follows the order 5-NMOH < MOH < 5-BMOH.

## References

1. Khamis E, Bellucci F, Latanision RM, El Ashry ESH (1991) Corrosion 47:677
2. Quraishi MA, Khan MAW, Jamal D, Ajmal M, Murlidharan S, Iyer SVK (1996) J Appl Electrochem 26:1253
3. Quraishi MA, Khan MAW, Jamal D, Ajmal M, Murlidharan S, Iyer SVK (1997) Br Corros J 32:72
4. Bentiss F, Traisnel M, Lagrenée M (2001) J Appl Electrochem 31:41
5. Wang HL, Liu RB, Xin J (2004) Corros Sci 46:2455
6. Behpour M, Ghoreishi SM, Soltani N, Salavati-Niasari M (2009) Corros Sci 51:1073
7. Yurt A, Bereket G, Kivrak A, Balaban A, Erk B (2005) J Appl Electrochem 35:1025
8. Fouad AS, Mahfouz H (2009) J Chil Chem Soc 54:302
9. Fouad AS, Mostarfa HA, El-Taib F, Elewady GY (2005) Corros Sci 47:1988
10. Damaskin BB, Frumkin AN (1971) In: Hush NS (ed) Adsorption of molecules on electrodes. Wiley-Interscience, London, p 1
11. Prabhu RA, Shanbhag AV, Venkatesha TV (2007) J Appl Electrochem 37:491
12. Li X, Deng S, Fu H, Li T (2009) Electrochim Acta 54:4089
13. Langrenée M, Mernari B, Bouanis M, Traisnel M, Bentiss F (2002) Corros Sci 44:573
14. Abd ElRehim SS, Hassan HH, Amin MA (2004) Corros Sci 46:25
15. Ramesh S, Rajeswari S (2005) Corros Sci 47:151
16. Lazarova E, Petkova G, Iankova T, Ivan L, Neikov G (2008) J Appl Electrochem 38:1391
17. Saukaitis A J, Gardner G S (August 14, 1970) US Patent, Derivatives of rosin amines 2:758,970
18. Gardner G S, Saukaitis A J (September 25, 1957) US Patent, Inhibitor acid 2:807,585
19. Quraishi MA (2003) Bull Electrochem 19:49
20. Sathisha MP, Revankar VK, Pai KSR (2008) Met Based Drugs. doi: [10.1155/2008/362105](https://doi.org/10.1155/2008/362105)
21. Karalı N (2002) Eur J Med Chem 37:909
22. Quraishi MA, Ahamad I, Singh AK, Shukla SK, Lal B, Singh V (2008) Mater Chem Phys 112:1035
23. Mathur PB, Vasudevan T (1982) Corrosion 38:171
24. Bockris JO'M, Drazic D (1962) Electrochim. Acta 7:293
25. Xu Li, Tang L (2005) Mater Chem Phys 90:286
26. Noor EA, Al-Moubarak AH (2008) Mater Chem Phys 110:145
27. Larabi L, Benali O, Harek Y (2007) Mater Lett 61:3287
28. Szauer T, Brandt A (1981) Electrochim Acta 26:253
29. Ghosh PK, Guhasarkar DK, Gupta VS (1983) Br Corros J 18:287
30. Agrawal YK, Talati JD, Shah MD, Desai MN, Shah NK, Putilova IK, Balezin SA, Barasanik YP (1960) Metallic corrosion inhibitors. Pergamon Press, Oxford, p 30
31. Abdallah M (2002) Corros Sci 44:717
32. Schorr M, Yahalm J (1972) Corros Sci 12:867
33. Clark PN, Jakson E, Robinson M (1979) Br Corros J 14:33
34. Riggs OL Jr, Hurd RM (1967) Corrosion 23:252
35. Damborenea JD, Bastidas JM, Vázquez AJ (1997) Electrochim Acta 42:455
36. Durrie W, Marco RD, Jefferson A, Kinsella B (1999) J Electrochem Soc 146:1751
37. Abd El-Rehim SS, Refaei SAM, Taha F, Saleh MB, Ahmed RA (2001) J Appl Electrochem 31:429
38. Yurt A, Balaban A, Kandemir SU, Bereket G, Erk B (2004) Mater Chem Phys 85:420
39. Badr GE (2009) Corros Sci. doi: [10.1016/j.corsci.2009.06.017](https://doi.org/10.1016/j.corsci.2009.06.017)
40. Tang L, Li X, Si Y, Mu G, Liu GH (2006) Mater Chem Phys 95: 26
41. Aljourani J, Raeissi K, Golozar MA (2009) Corros Sci 51:836
42. Keles H, Keles M, Dehri I, Serindag O (2008) Colloids Surf A Physicochem Eng Aspects 320:138
43. Singh AK, Quraishi MA (2009) Corros Sci. doi: [10.1016/j.corsci.2009.07.011](https://doi.org/10.1016/j.corsci.2009.07.011)
44. Moretti G, Quartarone G, Tassan A, Zingales A (1996) Electrochim Acta 41:1971
45. Tang L, Mu G, Liu G (2003) Corros Sci 45:2252
46. Li X, Deng S, Fu H, Mu G (2009) Corros Sci 51:620
47. Aljourani J, Raeissi K, Golozar MA (2009) Corros Sci 51:1836
48. Tao Z, Zhang S, Li W, Hou B (2009) Corros Sci. doi: [10.1016/j.corsci.2009.06.042](https://doi.org/10.1016/j.corsci.2009.06.042)
49. Lenderink JW, Linden M, Wit JH (1993) Electrochim Acta 38: 1989
50. Oguzie EE, Li Y, Wang FH (2007) Electrochim Acta 53:909
51. Qu Q, Jiang S, Bai W, Li L (2007) Electrochim Acta 52:6811
52. Lopez DA, Simison SN, Sanchez SRD (2003) Electrochim Acta 48:845
53. Lebrini M, Lagrenée M, Vezin H, Traisnel M, Bentiss F (2007) Corros Sci 49:2254
54. Hassan HH (2006) Electrochim Acta 51:5966
55. Riggs OL Jr (1973) Corrosion inhibitors, 2nd edn. C.C. Nathan, Houston, TX
56. Ferreira ES, Giancomelli C, Giacomelli FC, Spinelli A (2004) Mater Chem Phys 83:129
57. Olivares O, Likhanova NV, Gomez B, Navarrete J, Llanos-Serrano ME, Arce E, Hallen JM (2006) Appl Surf Sci 252:2894
58. Ostovari A, Hoseinieh SM, Peikari M, Shadizadeh SR, Hashemi SJ (2009) Corros Sci 51:1935
59. Schweinsberg DP, George GA, Nanayakkara AK, Steiner DA (1988) Corros Sci 28:33
60. Shorky H, Yuasa M, Sekine I, Issa RM, El-Baradie HY, Gomma GK (1998) Corros Sci 40:2173
61. Singh AK, Quraishi MA, (2009) Corros Sci. doi: [10.1016/j.corsci.2009.08.050](https://doi.org/10.1016/j.corsci.2009.08.050)
62. Noor EA (2005) Corros Sci 47:33
63. Bentiss F, Jama C, Mernari B, Attari HEL, Kadi LEI, Lebrini M, Traisnel M, Lagrenée M (2009) Corros Sci 51:1628
64. Donald MK Jr (1990) Chem Rev 90:585
65. Snyder BS, Patterson GS, Abrahamson AJ, Holm RH (1989) J Am Chem Soc 111:5214
66. Elayyachy M, Idrissi AEI, Hammouti B (2006) Corros Sci 48: 2470
67. Lece HD, Emregul KC, Atakol O (2008) Corros Sci 50:1460
68. Shriver DF, Atkins PW, Langford CH (1994) Inorganic chemistry, 2nd edn. Oxford University Press, Oxford, p 239